SHRP-I-622

Development of Metallic Coatings for Corrosion Protection of Steel Rebars

Angel Sanjurjo, Sam Hettiarachchi,
Kai Lau, Bernard Wood, and Philip Cox

Materials Research Center
Materials and Chemical Engineering Laboratory

SRI International
333 Ravenswood Avenue
Menlo Park, CA 94025

Strategic Highway Research Program
National Research Council
Washington, DC 1993

PUBL. NO. SHRP-I-622
Contract ID-023

Program Manager: *K.T. Thirumalai*
Project Manager: *Marty Laylor*
Production Editor: *Marsha Barrett*
Program Area Secretary: *Ann Saccomano*

January 1993

key words:

Strategic Highway Research Program
National Academy of Sciences
2101 Constitution Avenue N.W.
Washington, DC 20418

(202) 334-3774

Acknowledgments

The research described herein was supported by the Strategic Highway Research Program (SHRP). SHRP is a unit of the National Research Council that was authorized by section 128 of the Surface Transportation and Uniform Relocation Assistance Act of 1987.

Abstract

This report demonstrates the feasibility of applying a silicon-based diffusion coating on steel rebars, wires and fibers in fluidized beds of Si particles. In comparison to fusion-bonded epoxy coatings, or galvanized bars, the silicon coated samples indicate a higher corrosion resistance in aggressive chloride environments. In addition, the less expensive silicon-coated samples resist scratching.

Contents

Executive Summary

Compact and homogeneous silicon and silicon-titanium protective diffusion coatings were deposited on steel rebars, wires, and fibers by using a novel chemical vapor deposition technique. This technique combines the low cost of pack metallization with the advantages of subhalide chemistry and the high heat and mass transfer rates of a fluidized bed reactor. In this technique, the steel samples are immersed for a few minutes in a bed of silicon or silicon-titanium particles fluidized by using an argon/0.1% HCl gas mixture and kept at temperatures ranging from 400° to 750°C. Diffusion coatings were obtained in all cases with coating rates up to 1 μm per minute obtained at the highest temperatures. Multiple samples can be coated at the same time, and continuous coating and scaleup are envisioned for the next phase of work.

Selected coated samples were tested for corrosion resistance by chemical and electrochemical techniques. Silicon provided increased corrosion protection as expected. AC impedance measurements in acidic chloride solutions indicated that 1- to 5-μm-thick diffusion coatings were more protective than either very thin (<1 μm) or very thick (>10 μm) silicon diffusion coatings. The best results were obtained when Si and Ti were codeposited at temperatures around 550°C. These diffusion coatings increased corrosion resistance by more than an order of magnitude over that observed for the uncoated sample.

Preliminary bend tests on silicon-coated steel wires (0.125-inch o.d.) showed no cracks on the thin coatings with 90-degree bends. These coatings are much harder and more difficult to scratch than polymeric coatings. Preliminary comparative cost estimates indicate a lower cost for Si-Ti coatings than for polymeric coatings.

Contents

1

Introduction

The corrosion of steel rebars used for reinforced concrete structures such as bridges can be accelerated by a variety of agents. For example, Cl^- ions (arising from deicing salts or marine environments) diffuse rapidly through the concrete and cause the initiation of steel corrosion. The stresses created by the increase in volume which results from the formation of corrosion products, can lead to cracking of the concrete. Once corrosion has started, several approaches can be used to minimize its effects. Several of these approaches are currently being studied in research funded by the Strategic Highway Research Program (SHRP) and others (1). Current corrosion protection practices involve the use of cathodic protection (CP) systems, and the use of additives in concrete.

Because of the inherent problems associated with rebar corrosion resulting from Cl^- ion ingress into concrete, the use of other methods to protect is very important. The most common method consists of coating the rebar with fusion-bonded epoxies. Fusion-bonded epoxy coatings, although twice as expensive as uncoated black bars, have shown some corrosion resistance but are prematurely failing, especially, in subtropical marine environments such as the Florida Keys. Other disadvantages are that they can be easily scratched during handling and can debond once in use.

In some cases galvanized coatings are used. Galvanized bars show good corrosion resistance, but their zinc coating gradually corrodes as a result of its action as a sacrificial anode. When the zinc has been sacrificed, the rebar behaves like black rebar. Thus, in the long term, galvanized bars may have only a limited advantage over simple black bars.

In search for a better solution, researchers have explored the possibility of imparting better corrosion resistance properties to the steel by alloying it with protective elements. It is well known that adding Si to metals and alloys, including steel, generally increases their corrosion, oxidation, and erosion resistance (2). For example, Duriron, a commercial available alloy with a composition of 14% Si, provides significant corrosion protection (3). Because adding Si changes the bulk mechanical properties and increases the cost of the steel, we proposed coating the original steel rebar with a thin layer of corrosion-resistant material. This coating approach results in a diffusion-

coating which has been used for both ambient- and high-temperature corrosion and oxidation protection on a variety of substrates including ferrous alloys (4,5). Even greater protection can be achieved if the steel is coated with Ti, which is well known for its excellent corrosion resistance in chloride environments (3). Note that while polymeric coatings are soft and they bond weakly to steel rebars, Si diffuses into the steel forming a hard surface alloy which is an integral part of the rebar. Ti being a large atom, tends to stay in the surface forming a thin, Ti-rich, coating which is strongly adherent through metal-metal bonds.

Although many coating techniques such as chemical vapor deposition (CVD), physical vapor deposition (PVD), powder slurry, pack cementation, sputtering, and molten salts have been used to coat steel bodies, only a few satisfy the requirement of being able to produce a compact, low-cost coating that can conform to the surface of the substrate. CVD and pack cementation are frequently used in industry, however, conventional CVD is, in general, too expensive for low-cost industrial applications and requires relatively high deposition temperatures. Pack cementation requires high temperatures and long coating times (1000°C for 1 hour or more), which limits its use to substrates that can be exposed to the high temperature without degradation of their mechanical properties. Recently, several authors (5-9) have used coating chemistries that allow siliconization at much lower temperatures. Cabrera and Kirner (8) used SiH_4 in a CVD reactor which can siliconize iron at temperatures ranging from 500° to 600°C in 8-15 minutes, which significantly increasing the corrosion resistance to HCl and H_2SO_4 (Table 1). The major disadvantage of this approach is that SiH_4 is a very expensive source of silicon.

SRI International has recently developed a fluidized bed CVD technique that may satisfy the requirements of low cost and low temperature for depositing inorganic coatings that can substantially increase the lifetime of materials used in aggressive aqueous environments (7). In this project this coating technique is adapted to increase the corrosion resistance of steel used for concrete reinforcement. Briefly, the technique consists of immersing the surface in a fluidized bed of Si or Ti particles. The bed is fluidized with Ar containing 1% vol HCl and kept at temperatures ranging from 400° to 650°C. Reactive halosilane or subhalide species are generated *in situ* by the reaction of the HCl with the Si or Ti particles and it is these gaseous species which act as transport agents to deposit the Si or Ti on the substrate. The Si and Ti atoms may partially diffuse into, or stay on top of the substrate depending on the relative rates of deposition and solid state diffusion.

In this report, the experimental results obtained on steel rebars with beds of Si particles and mixtures of Si and Ti particles are described. We chose to deposit Si and Si-Ti coatings because of their proven capability for corrosion protection in Cl^- environments. Some advantages of this approach include simplicity of application, low cost, strong adherence, and chemical compatibility of the coating with concrete because of its natural oxidation to silicon dioxide (SiO_2) and TiO_2. Because of this compatibility, we expect high bond strength between the silicon-titanium-silica-titania-coated rebars and the concrete matrix. Therefore, our main objective is to coat rebar with corrosion-resistant silicon-titanium material to significantly lengthen the lifetime of steel-reinforced structures without any detrimental effects on the steels structural properties.

Table 1. Corrosion results[a]

Sample	Corrosion in HCl, 1N, 21°C	
	Current density (mA/cm^2) at V = 0	Corrosion Rate (Units/Year)
Uncoated Fe	1.07	494
Si coated at 500°C, 15 min.	0.38	135
Si coated at 600°C, 8 min.	0.39	138
Si coat 600°C, 15 min.	0.10	112
Duriron (14.5% Si)	0.03	

Sample	Corrosion in 72% H_2SO_4	
	Current density (mA/cm^2) at V = 0	Corrosion Rate (Units/Year)
Uncoated Fe	1.28	133
Si coated at 500°C, 15 min.	0.07	22
Si coated at 600°C, 8 min.	0.05	17
Si coat 600°C, 15 min.	0.10	34
Duriron (14.5% Si)	0.03	1

a. Cabrera et al., 1989, 1991; Cabrera and Kirner, 1989.

2

Technical Approach

Si and Ti diffusion coatings can be deposited by an SRI proprietary fluidized bed CVD coating technique that operates at atmospheric pressure and uses an *in situ* generated Ti-subhalide and halosilane chemistry to lower the deposition temperature (7,9). This technique combines the low cost of pack metallization with the high heat and mass transfer rates of a fluidized bed reactor (FBR) to produce homogeneous, compact, and conformal coatings.

The coating material (silicon or a mixture of Si and Ti) is loaded as a powder into an FBR (Figure 1). The powder is coated with CuCl, which acts as a catalyst and an inert gas is used to fluidize it. The system is heated to operating temperature, and the sample to be coated is immersed in the bed. Vapors of a halide species such as HCl are mixed with the inert fluidizing gas and react with the particles in the bed to produce halide species of the coating material (the chemistry is described in detail in the next section). By reacting with or disproportionating (breaking down and depositing metal) on the substrate, these species form the desired coating.

The cost of the reagents is relatively low in comparison with that of the reagents needed for CVD applications at low temperatures. Because the substrate is immersed in a fluidized bed and exposed to reactive gaseous species, all surfaces of complex shapes are coated more homogeneously than obtained from powder-pack or CVD techniques. The simplicity, predicted low cost of application, and flexibility of this technique make it very promising for increasing the corrosion resistance of steel in aqueous or nonaqueous environments.

In this project, the best conditions for generating the coating species in the fluidized bed were determined. Thermochemical estimates and mass spectrometry were used to determine the composition in the gas phase bathing the bed. Then, the kinetics of the reaction of HCl with the particles in the bed were studied. This information was used to select the best coating conditions and to actually coat steel samples. Finally, several corrosion and mechanical tests were performed to demonstrate the quality of the coatings.

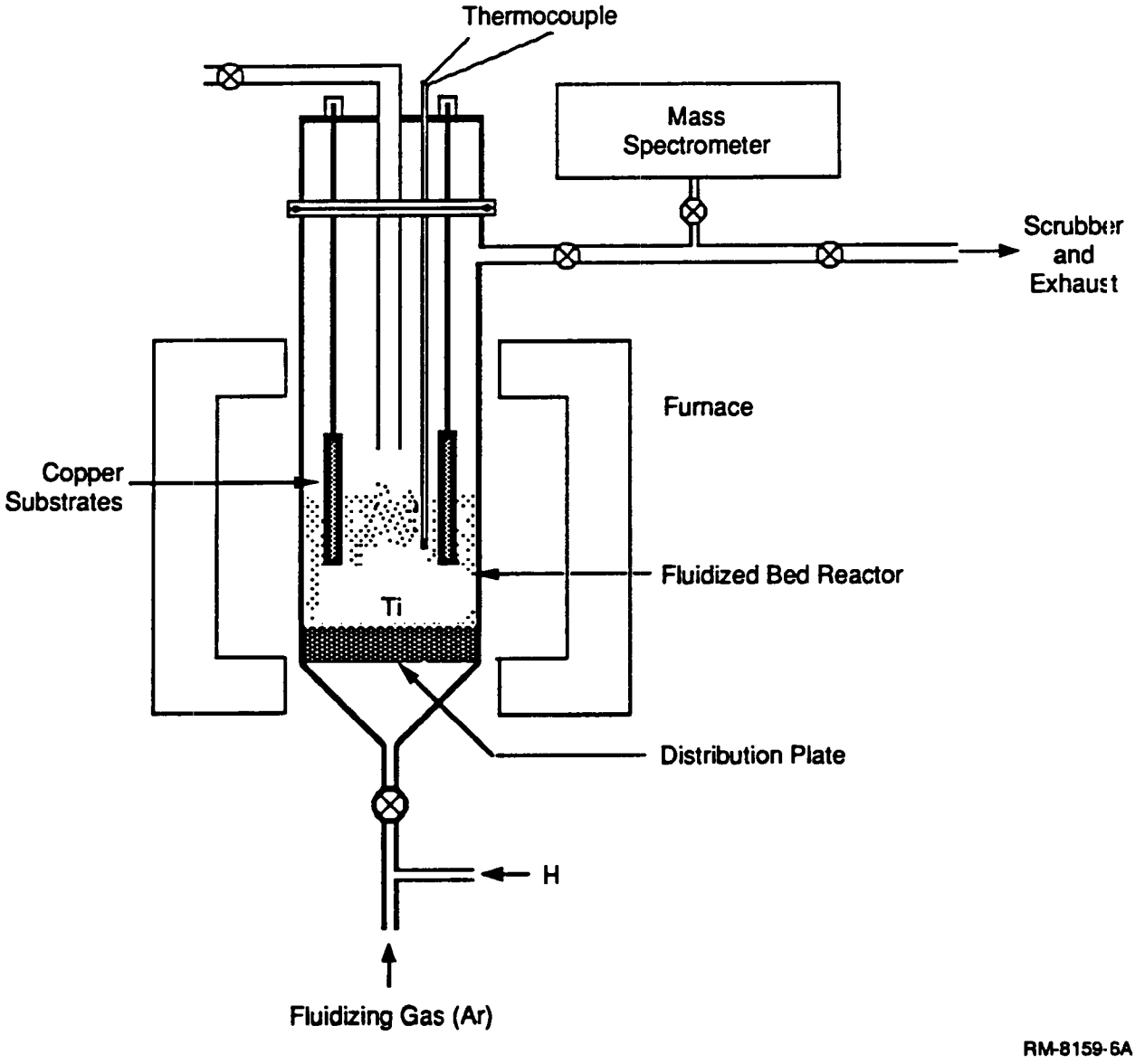

Figure 1. FBR for coating Si on steel.

Thermochemical and Kinetic Considerations

Chemistry in Silicon Beds

As HCl enters the fluidized bed of Si or Si-Ti particles, the overall mixture evolves toward equilibrium by following a path involving several reactions, including the formation of chlorosilanes according to

$$Si + 4HCl \leftrightarrow SiCl_4 + 2H_2$$

$$Si + 3HCl \leftrightarrow SiHCl_3 + H_2$$

$$Si + 2HCl \leftrightarrow SiH_2Cl_2$$

$$Si + 3HCl + H_2 \leftrightarrow SiH_3Cl$$

The main products are $SiHCl_3$, SiH_2Cl_2, and $SiCl_4$. SiH_3Cl is highly unstable and disproportionately breaks down instantly to form Si and SiH_2Cl_2. In addition, subhalides are also formed according to the following equations:

$$Si + 2HCl \leftrightarrow SiCl_2 + H_2$$

$$Si + SiCl_4 \leftrightarrow 2SiCl_2$$

$$Si + 3HCl \leftrightarrow SiCl_3 + 3/2\ H_2$$

$$Si + HCl \leftrightarrow SiCl + 1/2\ H_2$$

The lifetimes of SiCl and $SiCl_3$ are extremely short, and therefore they may not play an important role in coating. On the other hand, the lifetime of $SiCl_2$, although still short (~1 ms), is long enough for $SiCl_2$ to become an important coating species under the conditions of operation.

Thermochemical estimates of the vapor pressure of the gaseous species in equilibrium with Si have been made for a variety of temperatures, pressures, and Si/Cl and Cl/H values. Figure 2 shows the results of our estimates for the gas phase, assuming that excess Si is present. We have not included the Fe-Cl or the Cu-Cl species (from the substrate or catalyst) because they are not volatile at the temperatures of interest. We have used an updated set of thermochemical values, which are listed in Table 2, as the basis for the calculations.

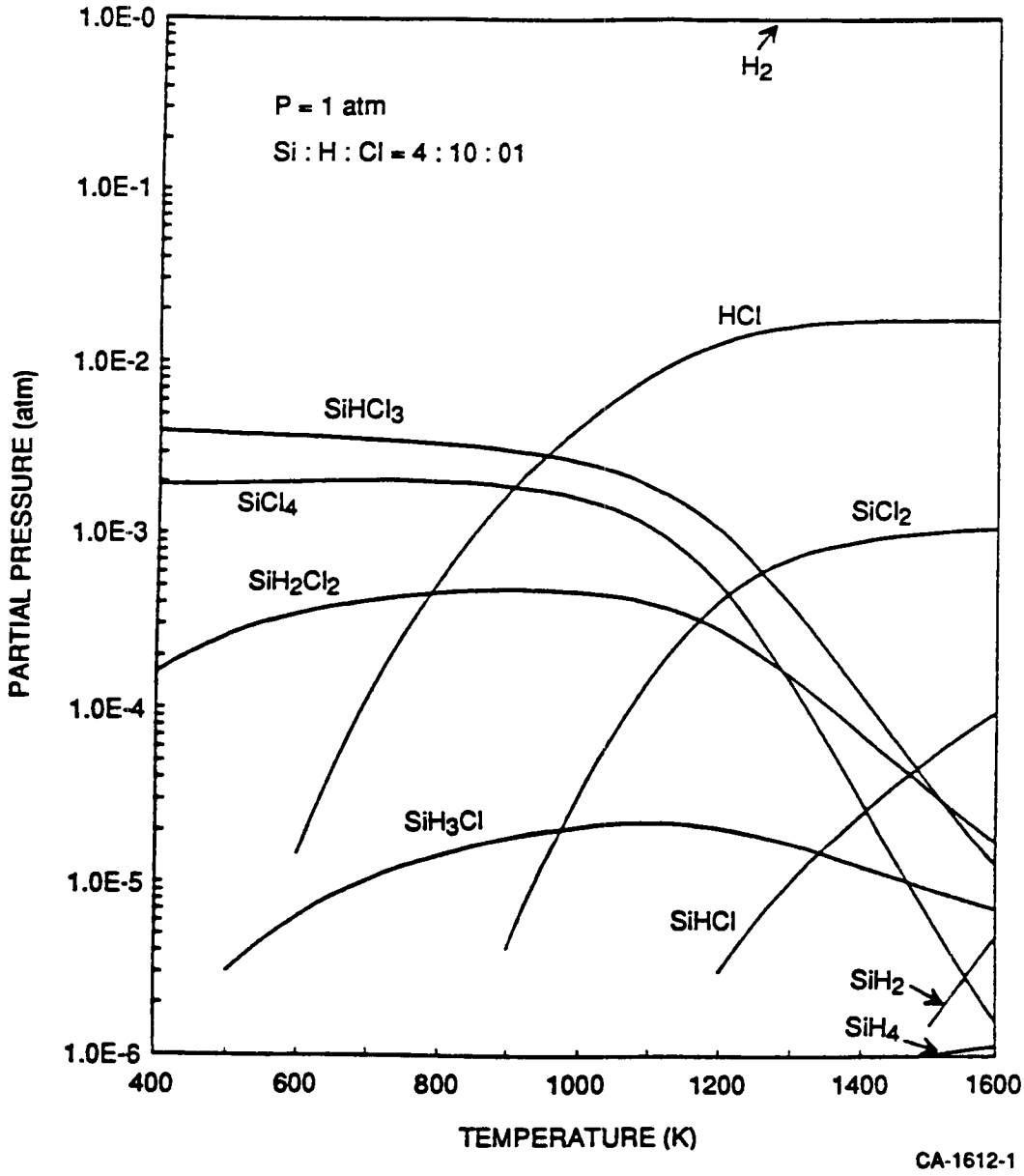

Figure 2. Equilibrium composition of the gaseous products of Si - H - Cl system at 1 atm total pressure.

Table 2. Selected heat values of formation and entropy at 1000K for various species in Si-Ti-Cl system.

Species	$\Delta_f H°_{298}$ (kJ/mol)	$S°_{1000}$ (J/mol/K)	Species	$\Delta_f H°_{298}$ (kJ/mol)	$S°_{1000}$ (J/mol/K)
Si	450.6	193.7	TiCl	169.0[a]	298.3[a]
SiCl	184.1[b]	282.4	$TiCl_2$	-228.9[a]	359.3[a]
$SiCl_2$	-168.6	348.2	$TiCl_3$	-539.3	415.2
$SiCl_3$	-326.4[b]	412.4	$TiCl_4$	-763.2	479.3
$SiCl_4$	-662.7	452.4	H	218.0	139.8
SiH	376.7	235.2	H_2	0.0	166.1
SiH_2	245.3[c]	263.3[c]	Cl	121.0	192.3
SiH_3	204.5[c]	280.9[c]	Cl_2	0.0	266.7
SiH_4	34.3	280.6	HCl	-92.3	222.8
SiHCl	40.9[c]	308.4[c]	Si(c)	0.0	47.3
$SiHCl_3$	-496.2	422.3	Fe(c)	0.0	66.7
SiH_2Cl_2	-320.5	383.3	$FeCl_2$(c)	-341.8	217.5
SiH_3Cl	-141.8	336.4	$FeCl_3$(c)	399.4	285.7
Fe	415.0	209.78	Ti(c)	0.0	64.7
FeCl	198.7[a]	304.8[a]	$TiCl_2$(c)	-515.5	181.0
$FeCl_2$	-136.0[a]	366.9[a]	$TiCl_3$(c)	-721.7	262.5
$FeCl_3$	-253.1	442.1	$TiCl_4$(l)	-804.2	431.3
Ti	472.8	207.3	TiH_2(c)	-144.3	90.3

a. D. L. Hildenbrand, SRI International, unpublished experimental data.
b. M. E. Weber and P. B. Armentrout, *J. Phys. Chem.* 93 (1989) 1596-1604.
c. V. P. Glushko, L. V. Gurvich, G. A. Bergman, I. V. Veitz, V. A. Medvedev, G. A. Kachkuruzov, and V. S. Yungman, *Thermodynamic Properties of Individual Substances*, Vol. I-IV, Academy of Sciences, Moscow, USSR (1982); English Edition, Vol. I-II (1991).

If $SiCl_4$ is used as the reactive species in H_2 atmospheres, its reduction to Si is not expected to be appreciable below 1000K. On the other hand, if HCl is injected, it is expected to react at lower temperatures to form the Si-Cl-H species, such as $SiHCl_3$, and SiH_2Cl_2.

In practice, however, our own kinetic studies and the work of many researchers in the semiconductor silicon industry have shown that HCl will react with pure Si only at high temperatures. Si will react with HCl at low temperatures if it is doped or catalyzed by impurities (10). Thus, adding the Cu catalyst results in a low-temperature reaction and promotes the formation of $SiHCl_3$, SiH_2Cl_2—and probably other less stable species such as $SiCl_2$ over that of $SiCl_4$—the most thermochemically stable species. The advantage of using the Cu catalyst is that these hydrogenated and unstable species produced *in situ* can be reduced or disproportionated on the steel surface to deposit Si at relatively lower temperatures.

These catalytic effects have been described previously in the scientific and patent literatures (10). The presence of some of these species in our coating reactor was confirmed by mass spectrometric analysis. The effect of temperature on the composition of stable species in the gas phase when pure or Cu-doped silicon reacts with $SiCl_4$ or HCl vapors was determined experimentally. For these studies, temperature-programmed reaction, a common technique in catalysis, was used. Briefly, Si powder is loaded into a microreactor in a fixed-bed configuration, as shown in Figure 3. The reacting gas is passed through the bed and the temperature is ramped at a constant rate. The composition of the gaseous product is monitored in real time by mass spectrometry.

It was found that when high-purity (99.999%) silicon was used, the reaction with HCl did not start until the temperature had reached 750°C (Figure 4a). The HCl signal clearly dropped at this temperature, and the Si-H-Cl species signal increased. In contrast, when metallurgical-grade silicon [98%, containing several thousand parts per million by weight (ppmw) of Fe and Al and hundreds of ppmw of other transition metals] was used, the reaction with HCl to form halosilanes started at 350°C (Figure 4b). When Cu-coated Si particles were used in the bed, HCl began to react at 250°C, as shown in Figure 4c. This condition, therefore, seemed especially suited to our coating purposes, and it was used for coating the steel samples.

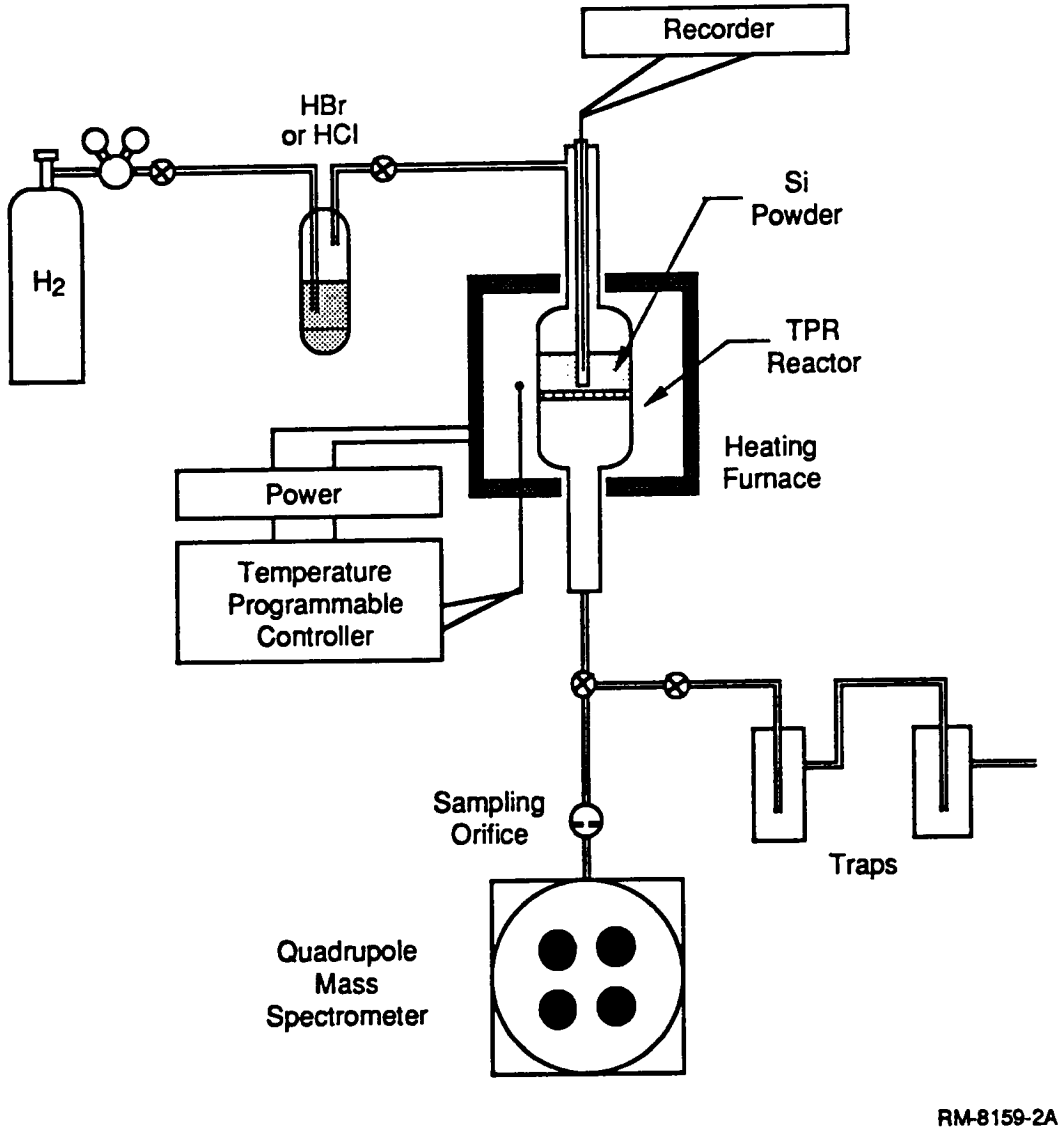

Figure 3. Schematic drawing of TPR system.

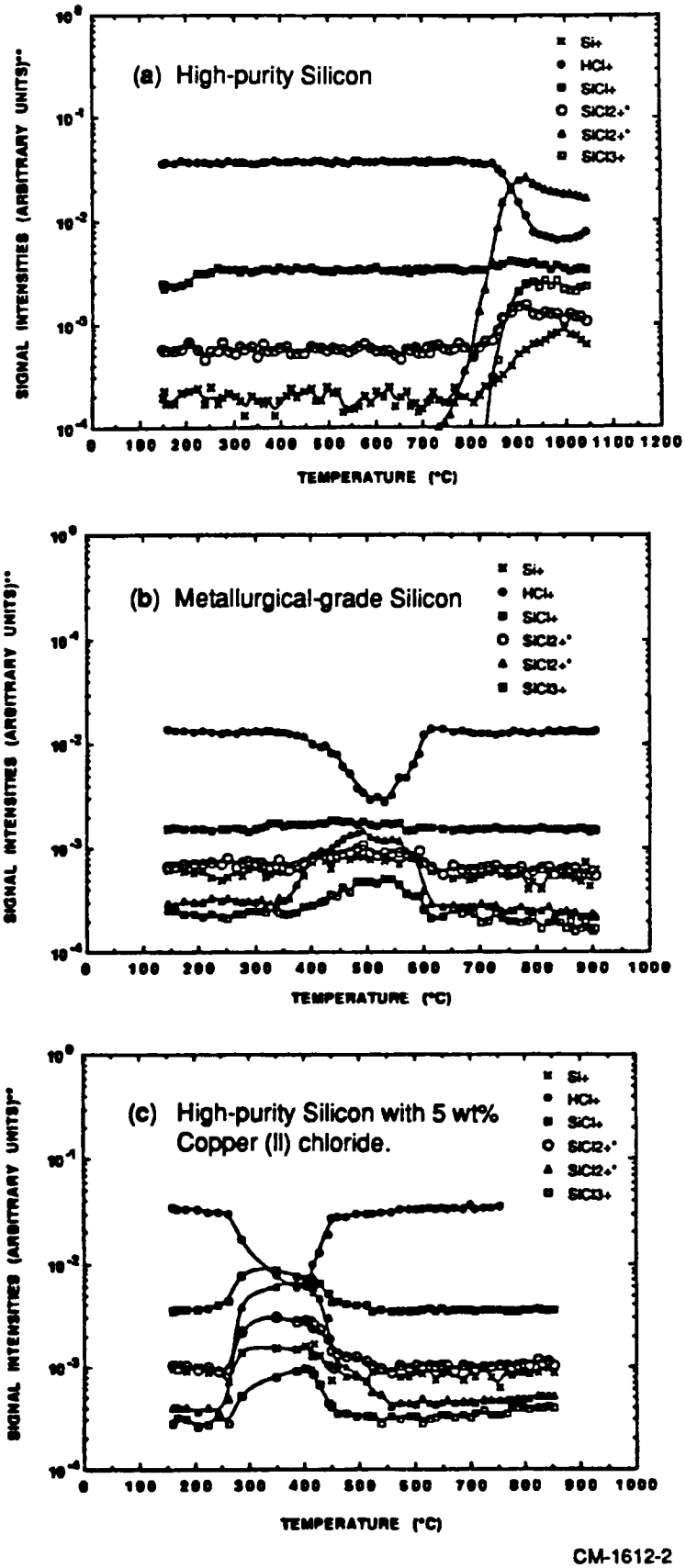

Figure 4. Temperature-programmed reactions in a hydrogen chloride/hydrogen mixture.

Chemistry in Titanium Beds

In this case, only the Ti subhalides and TiH_2 are formed according to equilibrium, such as

$$Ti + 4HCl \leftrightarrow TiCl_4 + 2H_2$$

$$Ti + 3HCl \leftrightarrow TiCl_3 + 3/2\ H_2$$

$$Ti + 2HCl \leftrightarrow TiCl_2 + H_2$$

$$Ti + TiCl_4 \leftrightarrow 2TiCl_2$$

$$Ti + 3TiCl_4 \leftrightarrow 4TiCl_3$$

The formation of $TiCl_3$ and $TiCl_2$ is expected to be the most important path for coating Ti, because these two subhalides can disproportionate or revert to Ti.

Thermochemical estimates were made of the partial pressures or mole fractions of gaseous and solid species in equilibrium in the Ti/Cu/Cl/H system at various temperatures, pressures, and values of the Ti/Cu/Cl/H ratio. As shown in Figure 5a, our calculations predict that $TiCl_3$ will be the principal gaseous species in contact with a Ti bed $T < 500K$ and $H/Cl = 10$.

The thermochemical analysis also indicates that TiH_2 will be the dominant solid-phase species at temperatures below 975 K (703°C) (Figure 5b), whereas Ti will be the dominant phase at $T > 975$ K (703°C). The other solid phases present—$TiCl_2$, $TiCl_3$, and Cu—remain at relatively constant levels in the temperature range of interest. Therefore, at 975 K (703°C) we can expect the Ti particles in the bed to be covered with a $TiCl_2$-$TiCl_3$-TiH_2 mixture, while $TiCl_3$ vapor is the principal constituent of the gas phase. If nitrogen is added to the gas phase, TiN will become the most stable phase in the temperature range of 925-1050 K (652°-777°C) (Figure 5c). In the absence of H, $TiCl_3$ becomes the predominant species in the gas phase at these temperatures.

The respective reaction rates of $TiCl_4$ and HCl with pure Ti, and then with Cu-treated Ti were measured by temperature-programmed reaction (TPR). As described above, the reactive vapor is passed through a fixed bed of the solid material in a microreactor while the reactor effluent is monitored using an on-line mass spectrometer. The bed temperature was raised at a constant rate, and the composition of the gaseous product was measured as a function of temperature. Of all the species in the Ti-Cl system, only $TiCl_4$

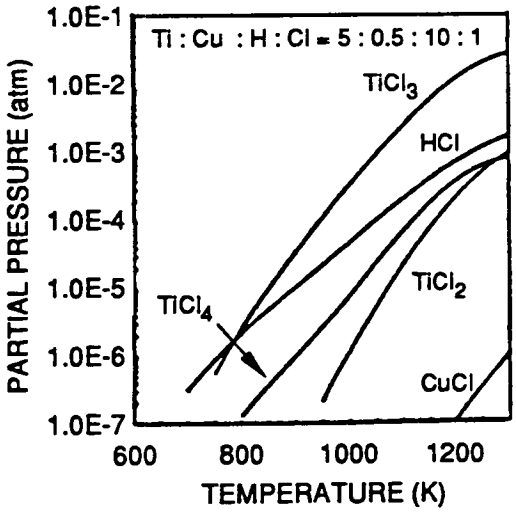

(a) Gaseous products of the Ti - Cu - H - Cl system

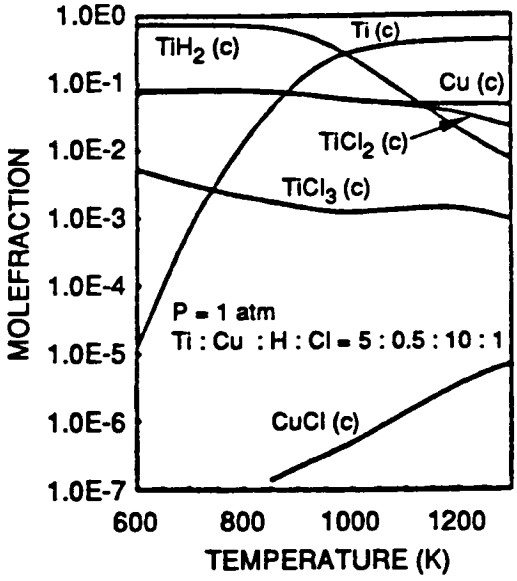

(b) Solid phase of the Ti - Cu - H - Cl system

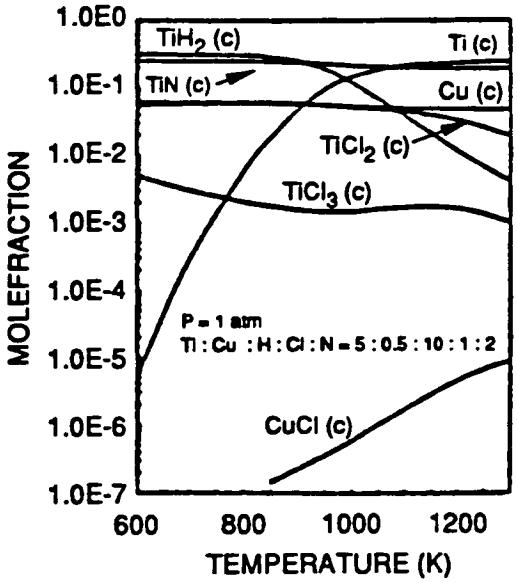

(c) Solid phase of the Ti - Cu - H - Cl - N system

CM-1612-3

Figure 5. Thermochemical estimates of equilibrium compositions for the Ti - Cl - H system at 1 atm total pressure.

vapors can reach the sampling inlet of the mass spectrometer kept at atmospheric pressure and room temperature. $TiCl_3$ and $TiCl_2$, even if produced in the reactor at high temperatures, would condense or disproportionate in the sampling probe. Therefore, the two $TiCl_2^+$ signals are also the result of fragmentation of $TiCl_4$. We found that with high-purity (99.9%) titanium, the reaction with $TiCl_4$-H_2 did not occur at a measurable rate at $T < 1100$ K (877°C), as shown by the decrease in the intensity of the $TiCl_3^+$ ion fragment, which is the major peak for $TiCl_4$ (Figure 6a). In contrast, the reaction of Ti particles with HCl becomes significant at 923 K (650°C), as shown in Figure 6b by a drop in the HCl and a rise in the $TiCl_3^+$ signals. When 5% $CuCl_2$ was added to the Ti particles in the bed, the reaction with HCl became observable at 723 K (450°C) (Figure 6c) and reached a maximum at about 873 K (600°C). Thus, $CuCl_2$ acts as a catalyst for the HCl-Ti reaction, rendering the system usable for low temperature of Ti in the fluidized bed reactor.

Chemistry in Beds of Si and Ti Powder Mixtures

Thermochemical estimates of the vapor pressure of the gaseous species in equilibrium with Si and Ti have been made for a variety of temperatures, pressures, and values for Si/Cl, Ti/Cl, Si/Fe/Cl, and Cl/H. The effect of temperature on the vapor pressures of the main species is shown in Figure 7. At up to 800 K, the pressures of the Si-Cl-H and Ti-Cl vapors increase with the temperature. Above 523°C (800 K), the pressures decrease, indicating that conditions are favorable for solid deposition.

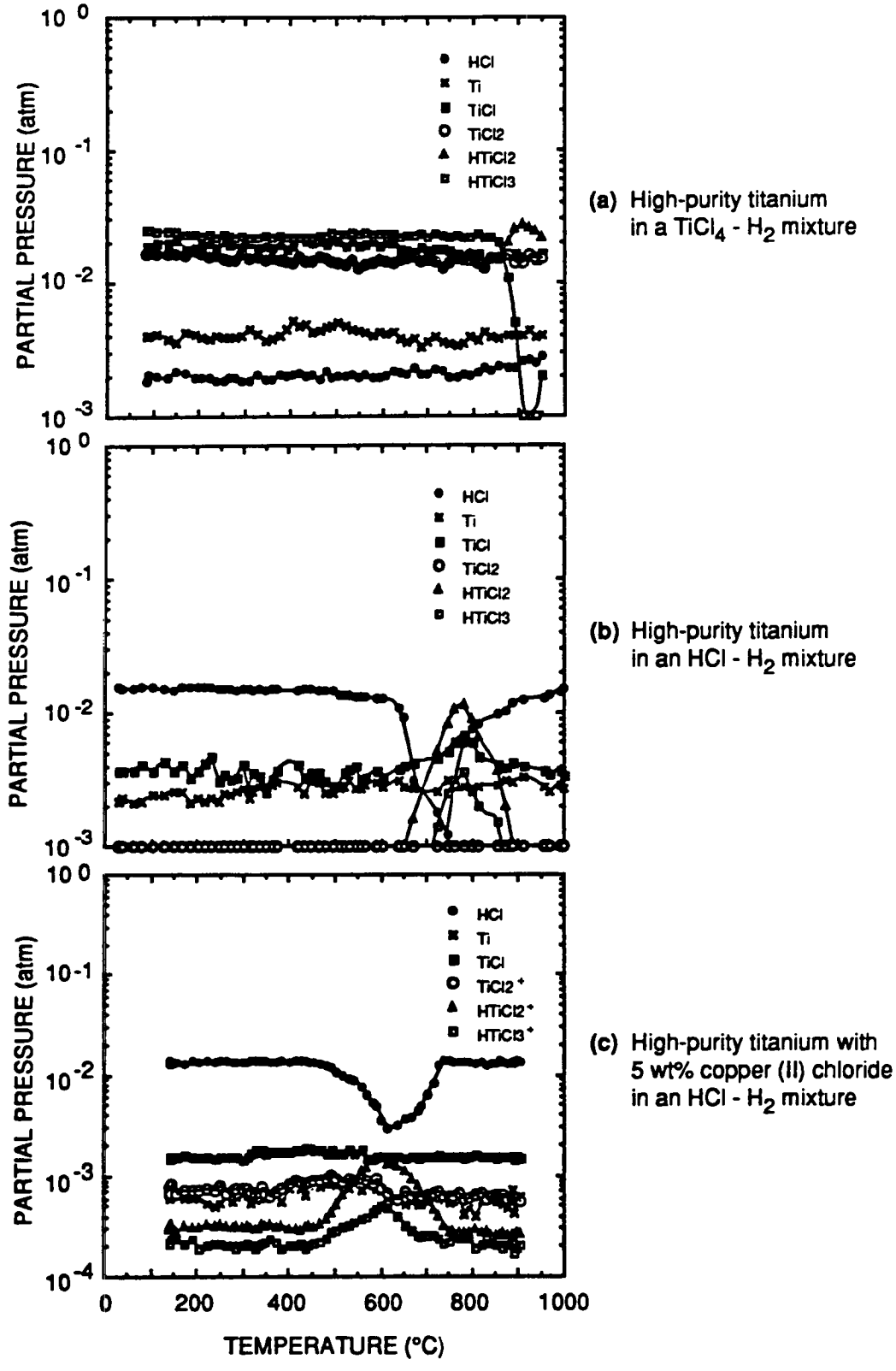

Figure 6. Effect of temperature and titanium purity on gas phase composition.

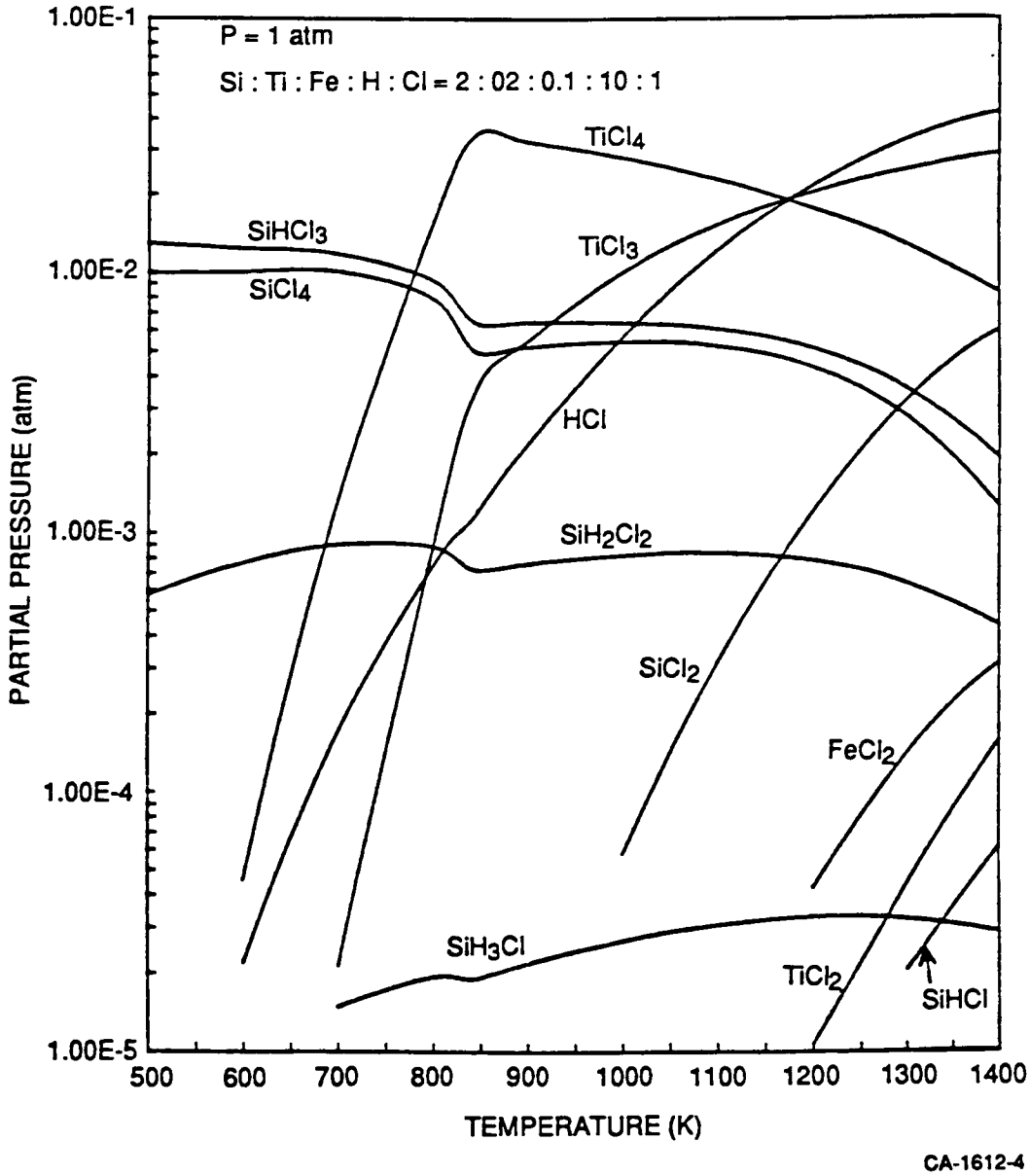

Figure 7. Equilibrium composition of the gaseous products of Si - Ti - Fe - H - Cl system at 1 atm total pressure.

Experimental Coating

Coating Procedure

Steel rebars (1.27 cm in diameter), Fe rods (0.30 cm in diameter), and sponges made of steel fibers (about 0.04 cm in diameter) were used as substrates. The as-received steel rebars were sandblasted to remove surface oxidation, then cut into 0.5- to 2-cm-thick disks. The disks were polished and etched in Nital (5% HNO_3/95% methanol) to characterize the microstructure of the as-received rebar material. Most grains range in size from 10 to 50 μm, as seen by scanning electron microscopy (SEM), (Figure 8).

Metallurgical grade silicon and/or titanium powder in particle sizes ranging from 250 to 500 μm was mixed with 5 wt% $CuCl_2$ catalyst and loaded into the quartz reactor to form a bed 10 cm high. The bed was fluidized by an inert gas (typically argon with a linear velocity of 10 cm s^{-1} in the laboratory operation). The reactor was heated to a bed temperature in the range of 250° to 650°C while a mixture of hydrogen and hydrogen chloride (partial pressure of HCl = 0.01 atm) was introduced into the fluidizing gas stream. Upon contact with the Si and/or Ti particles, these reactants form chlorosilane and silicon or titanium subchloride species that react or disproportionate on the steel substrate to deposit Si and/or Ti. The steel rebar coupons, steel rods, or steel fibers immersed in the fluidized bed attained the same temperature as the surrounding powder. Coating times of 1 to 120 minutes were tried. External heating by means of a resistance-heated tubular furnace or direct internal heating are used. In the latter case, external coils powered by a radio frequency power supply induct directly on the steel samples, which in turn heat the bed of particles.

Coating Results

We obtained diffusion-coatings in all our experiments. The conditions and results of the coating experiments are summarized in Table 3. All samples were allowed to cool either in Ar (which contains some O_2) or in a NH_3 atmosphere. Consequently, a thin film (20-40 Å) of oxides (SiO_2) or nitrides (Si_3N_4, TiN) was formed on the surface, protecting it further.

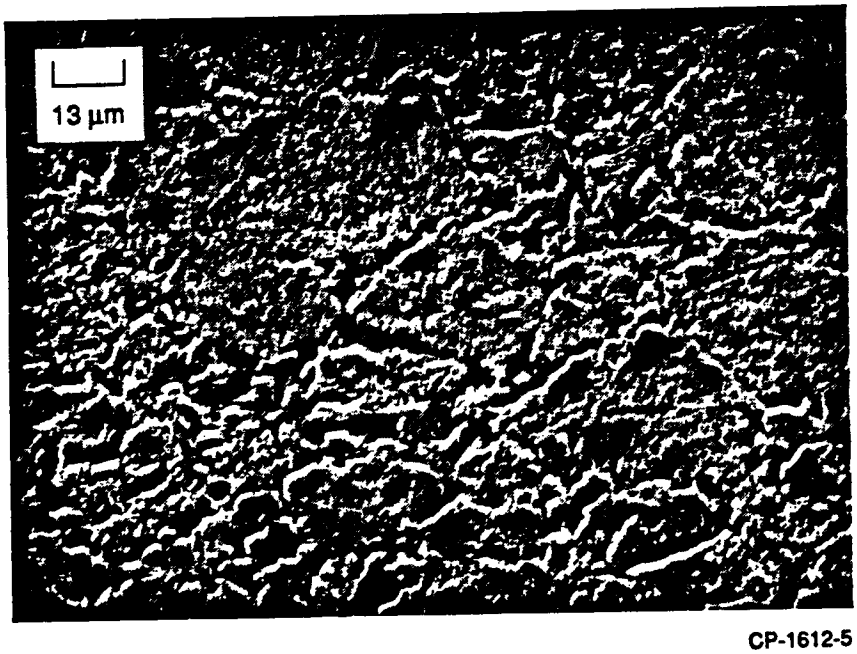

CP-1612-5

Figure 8. Microstructure of uncoated steel rebar as examined by SEM.

Table 3. Silicon and silicon-titanium coatings on steel

Substrate[a]	Coating	Temperature (°C)	Time (min)	Coating Characteristics
R	Si	700-750	60	Gray corrugated coat, 0.5 mm Top coating spalls off easily Si crystal deposition FeSi (X-ray diffraction)
R	Si	600-650	60	Gray corrugated/top coat spalls off Si crystalline deposit
R	Si	550	60	Smooth dark gray layer Adherent, no spallation Cooling rate 100°C/min Si crystals formed
R	Si	650	30	Top corrugated
R	Si	600	26	Layer = FeSi (X-rays) Midlayer = Fe_3Si
R	Si	600	9	Metallic gray - FeSi (X-rays)
R	Si	500	6	Si metallic dark gray Si_3N_4
R	Si + Ti	520	7	Si, Ti metallic dark gray TiN, Si_3N_4
R	Si + Ti	545	15	Si, Ti Gray + golden reflections
W	Si	<400	1,2,5,10	Substrate a-Fe (1%-2% Si Metallic gray coatings after 5 minutes
W	Si	450	2,4,8,16	Metallic gray Some oxidation observed
W	Si	550	2,4,8,16	Metallic gray, no oxidation
W	Si	650	2,4,8,16	Metallic gray, no oxidation
F	Si	~500	10	Metallic gray, no oxidation

a. R = rebar, W = wire, F = fiber.

Characterization of the Coatings

Composition, morphology, mechanical properties, and corrosion resistance were evaluated by a variety of techniques. The morphology and the composition were determined by a combination of optical microscopy, SEM, X-ray fluorescence (EDAX), Auger electron spectroscopy (AES), and X-ray diffraction (XRD) analyses. These tests were performed on the coated surfaces, as well as on cross sections of the samples, to determine the properties of both the coatings and the substrates. Bend tests were also performed to determine whether the coatings were flexible. Electrochemical corrosion was evaluated by the AC impedance technique.

Composition and Morphology

Silicon-Based Diffusion Coatings
At coating temperatures below 500°C, the coatings are adherent, compact, and conformal. A typical diffusion profile obtained by depth profiling and Auger spectroscopy is shown in Figure 9.

In short deposition time experiments (1-16 minutes), at 550°C, we observed that it takes approximately 5 minutes for the surface to turn grey. With the thinnest diffusion coatings (<0.1 μm) obtained in less than 5 minutes, this color fades after a few days of exposure to ambient air. By low magnification microscopy we observed that Fe-O islands grow out of isolated pinholes a few micrometers in diameter. Thicker Si coatings remain all gray even after bending and long periods of exposure (months) to the atmosphere (see Figure 10).

At deposition temperatures ranging from 500° to 600°C, Si-based coatings of 1 to 10 μm were obtained in 10 to 60 minutes. The general appearance is shown in Figure 11a. A cross-section view of another coated specimen shows a multilayered coating (Figure 11.b). The topmost layer and the underlying 10 μm have silicon in them. The inner band contained less than 1% silicon. It seems to be a recrystallization band, but the original steel microstructure remained intact 50 μm under the coating. The main portion of the external coatings was composed of Fe_3Si and FeSi (when Si was the only material) as determined by EDAX and Auger spectroscopy. The underlying substrate showed that up to 2% Si had diffused into it. A typical composition profile by EDAX is shown in Figure 12.

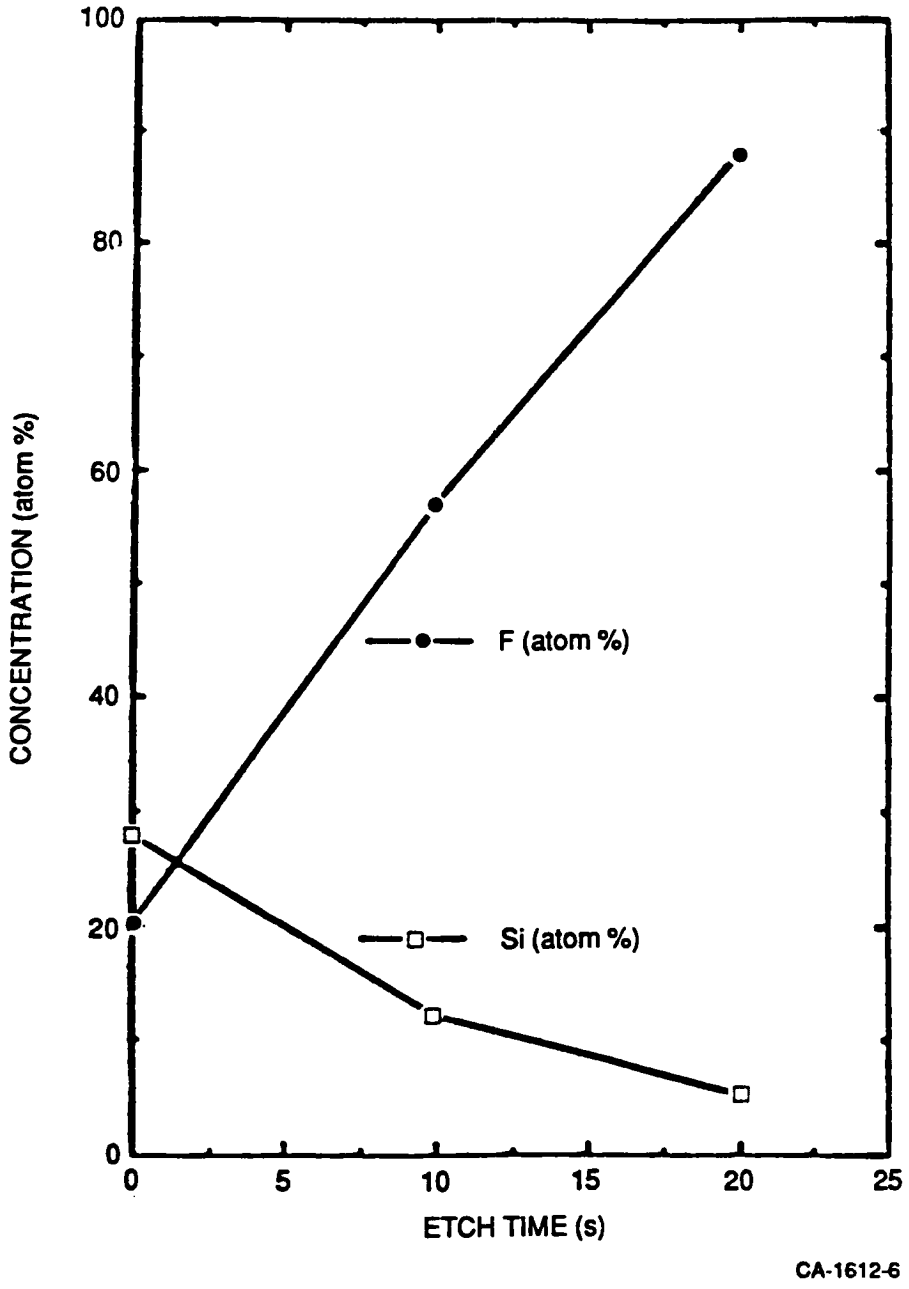

Figure 9. Concentration profile for coatings on steel fibers (500°C, 10 min).

Typically, silicon-based coatings obtained at higher temperatures (600° to 750°C) are multilayered and very thick (up to >100 μm), and the topmost corrugated layer spalls off. At 650°C (60 minutes deposition), thick multilayered corrugated coatings were deposited. A thick outer coating spalled off at some spots, revealing two other layers underneath (Figure 13a): a Fe-Si adherent layer, and a Si-doped steel substrate surface. Cross sections of similar samples showed that the Fe-Si layer was 20 μm thick, compact, and acid-resistant. The intermediate layer between the substrate and the outer layer was etched preferentially once the outer layer was removed (Figure 13b). The microstructure of the steel bar (top in Figure 13b) remained unchanged.

At 750°C we obtained an even thicker three-layer coating, including a 20-μm interdiffusion layer that had pores at some locations, a 30-μm intermediate compact layer, and a ~60 to 100-μm corrugated external layer. The general appearance and typical cross section are shown in Figure 14a, b. Crystallites of Si were deposited in some spots (Figure 14c). The interdiffusion layer adjacent to the substrate contains about 15 wt% Si and 85 wt% Fe, and the next layer contains about 24 wt% Si and 76 wt% Fe. The measured ratio of Si to Fe suggests that the interdiffusion layer is an Fe_3Si phase. The outer layers have an overall composition close to Fe_2Si, but X-ray diffraction shows only the top FeSi phase (Figure 15).

Although the original rebar structure did not change (Figure 14b) even in this time-temperature product, we did not pursue higher deposition temperatures. Diffusion depths of 10^2 μm have been reported for higher temperatures (4).

Si-Ti Coatings

When both Si and Ti were deposited, the thickness was <1 μm and there was no evidence of any compound formation. The temperature was 550°C, and deposition time was 30 minutes. The Si-Ti coatings have a bright surface similar to the one in Figure 11. SEM shows a compact adherent layer. X-ray diffraction does not detect any phase formed, and EDAX indicates that Si and Ti are each diffused in the Fe and the concentration is 2.5% by weight.

Mechanical Testing

Only preliminary bend and scratch tests were performed on some of the samples. Thin coating (<1 μm) showed no indication of spalling or cracking in 120° and 90-degree bend tests performed on 0.125 inches thick steel bars. Areas around notches made in the bars prior to coating did not show any sign of spallation or cracking as determined by optical microscopy and magnifications of up to 50 times (Figure 10).

The external layer of composite, thick (over 40 μm), Si-based, coatings could be easily scratched in some zones. The underlying Si-diffused layers were harder than the uncoated steel and cannot be detached without scratching the bulk of the substrate.

CP-1612-7

Figure 10. 90-Degree bends in Si-coated (top) and uncoated steel rods.

(a) Section of steel rebar Si-coated at 550°C for 60 min

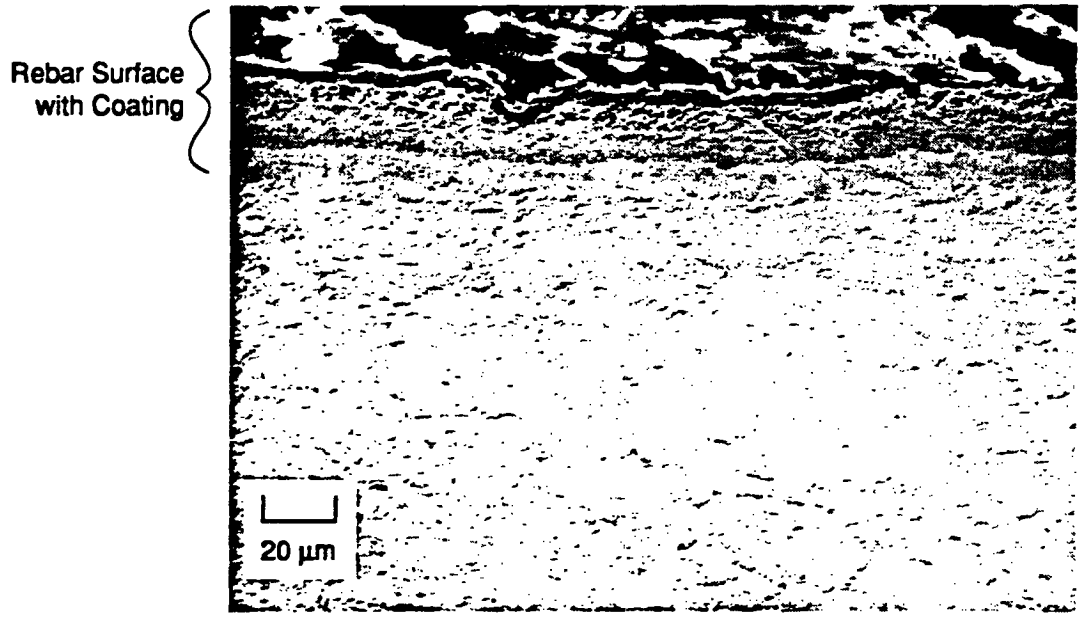

(b) Cross section of steel rebar Si-coated at 600°C for 30 min

CP-1612-8

Figure 11. Si-based coatings at T = 500°-600°C.

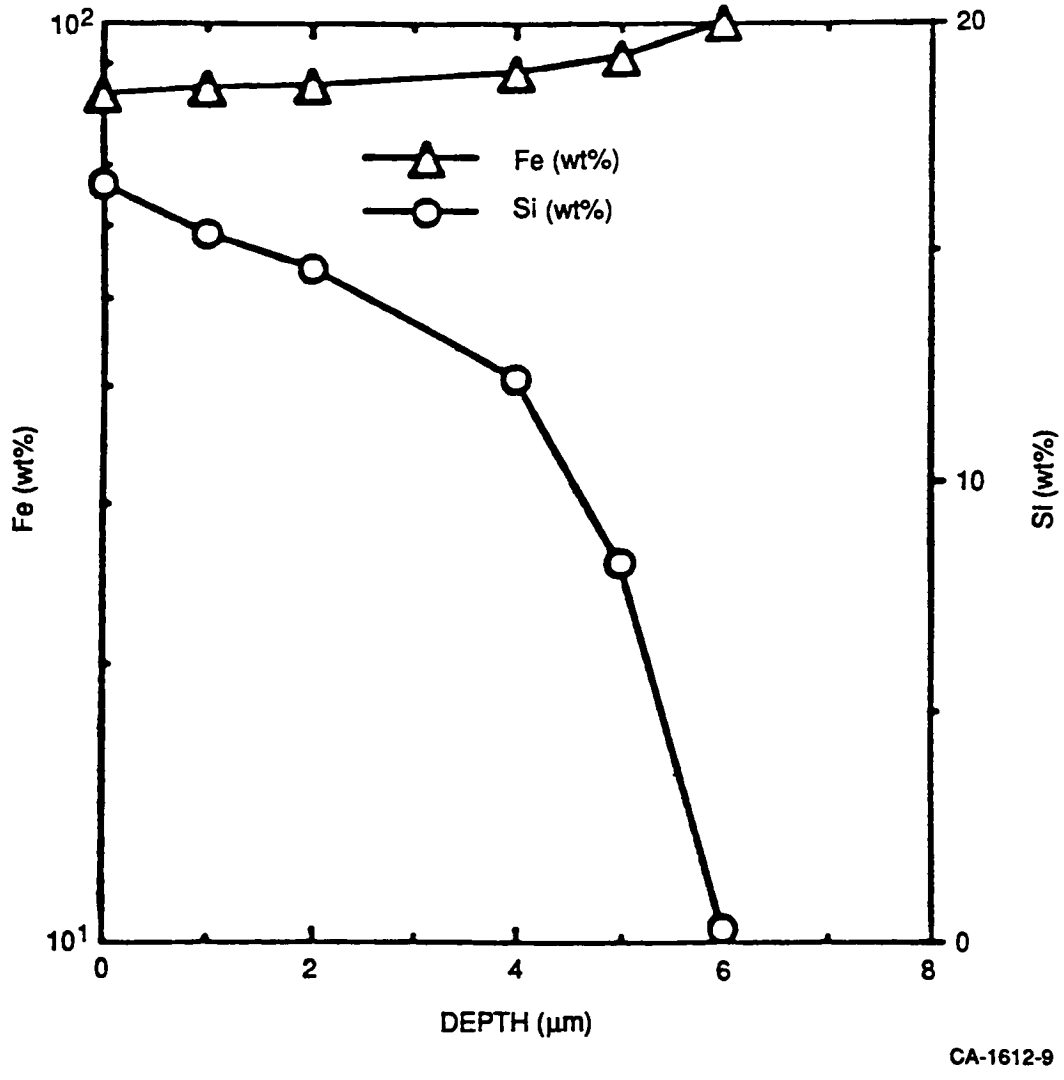

Figure 12. Si concentration profile for coatings on steel rods 600°C, 10 min.

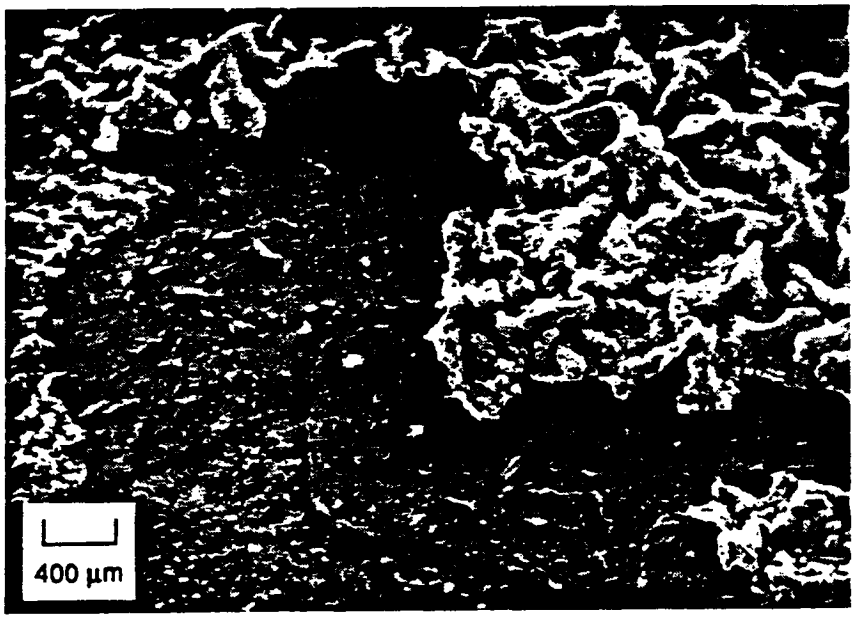

(a) General view

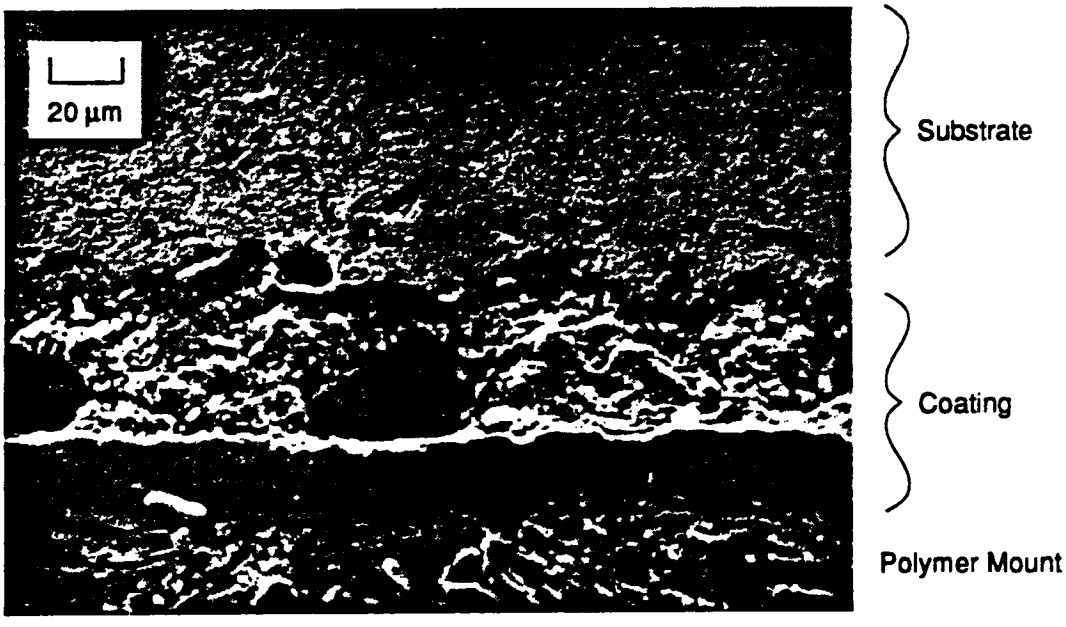

(b) Cross section

CP-1612-10

Figure 13. Steel rebar coated with silicon at 650°C during 60 min.

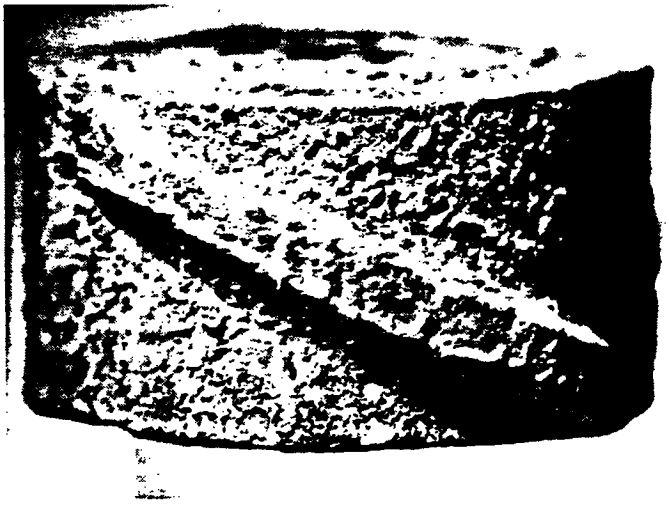

(a) General view

(b) Cross section

(c) Surface morphology

CP-1612-11

Figure 14. Si-coated steel rebars at 750°C, 60 min.

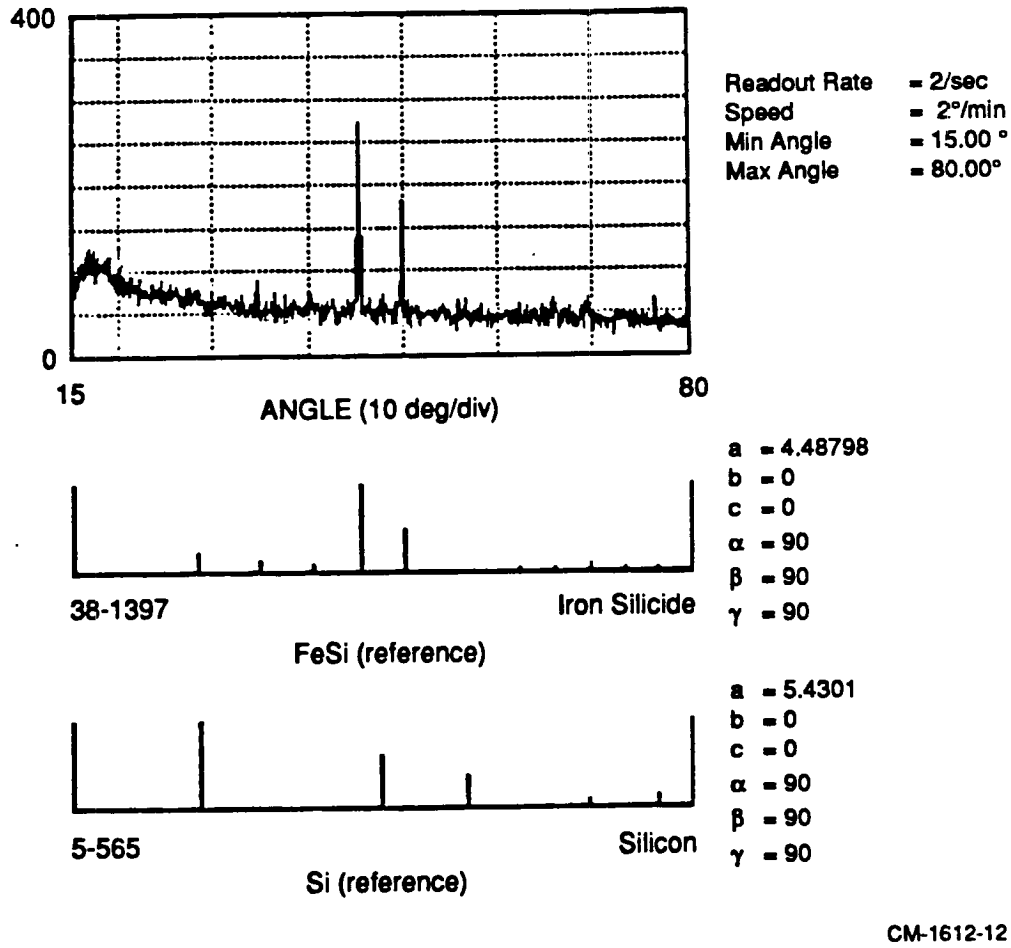

Figure 15. XRD pattern of steel coupon coated with silicon at 750°C.

Corrosion Resistance

The resistance to corrosion of the coated samples was tested by using an AC impedance measurement technique described in previous papers and reports to SHRP. Corrosion resistance of several coatings on sandblasted rebar was examined by using AC impedance techniques in a 5% sodium chloride electrolyte at pH 3.5. The sample was allowed to come to equilibrium in the test solution (30 minutes), and the impedance characteristics were examined at the open circuit (free corrosion) potential. Figure 16 is a schematic of the system used to compare the relative corrosion rates on coated and uncoated rebars. The real impedance or resistance to polarization R_p for uncoated rebar was about 150 Ω, versus 260 Ω for Si-coated and close to 1000 Ω for Si/Ti-coated rebars. Since R_p is inversely proportional to corrosion rate. This finding indicates that the corrosion rate relative to uncoated rebars should decrease to about 1/2 for Si-coated samples and to about 1/15 for Si/Ti-coated samples.

Figure 17 shows the impedance plot for the uncoated sandblasted bar. The response has a polarization resistance of approximately 160 Ω and a corrosion potential of -615 mV versus SCE (saturated calomel electrode). The sample appeared to show rapid general corrosion in this electrolyte, with iron dissolution over the entire rebar surface. No iron oxide corrosion products were observed on the surface after the impedance data were gathered.

Samples were coated with silicon at 650°C and the AC response was measured. The sample did not show the simple semicircular response expected from a freely corroding system, but instead two semicircles were observed. The sample had a relatively thick coating of silicon that, after being left in the electrolyte for approximately one hour, showed signs of porosity, and pinhole spots of iron oxide (rust) were observed on the surface. However, these pinholes were not located over the entire surface, and a large area of the surface showed no visible signs of corrosion. (The major areas of higher porosity and corrosion where the cut end of the rebar, which is not representative of the bulk rebar surface because of a high level of grain boundaries and imperfections, and the edges of the ribs in the rebar surface). This porosity is probably the cause of any mixed AC characteristics shown by the system in these short-term measurements.

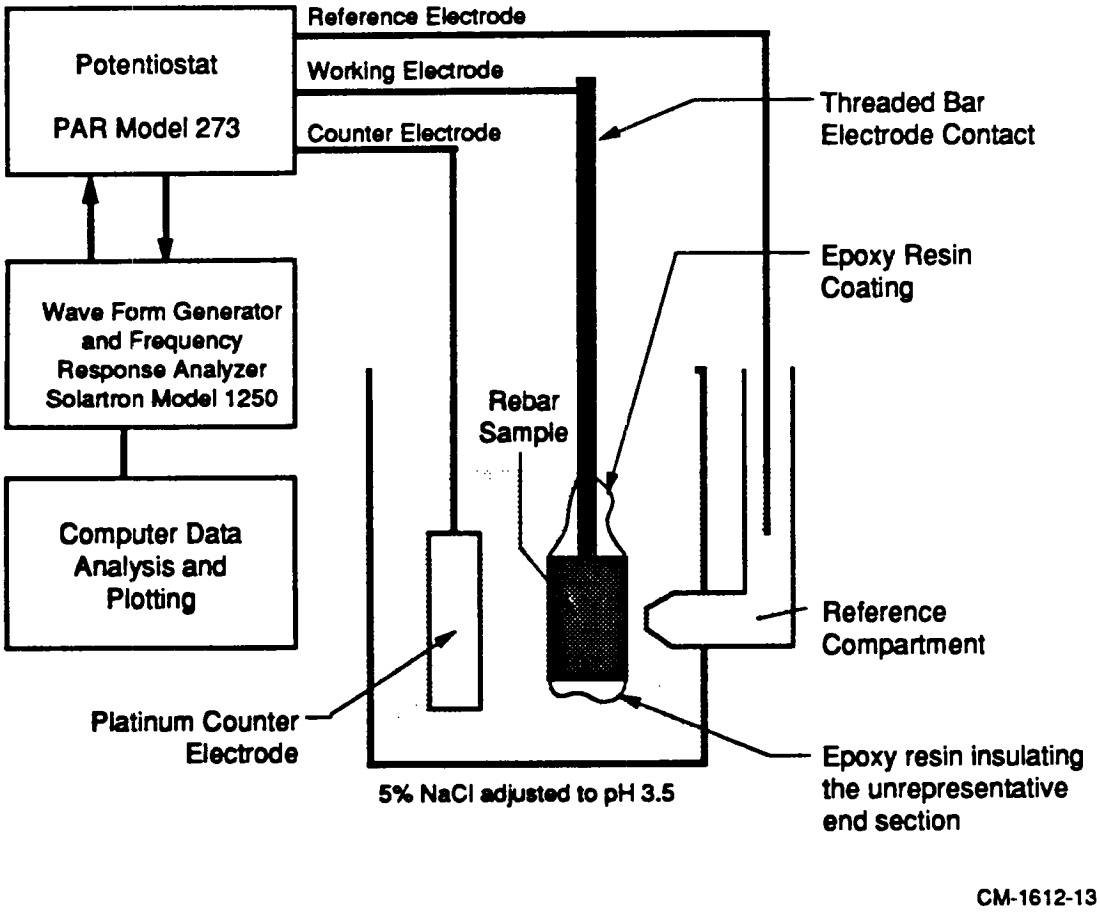

Figure 16. Schematic of AC impedance system to evaluate comparative corrosion tests.

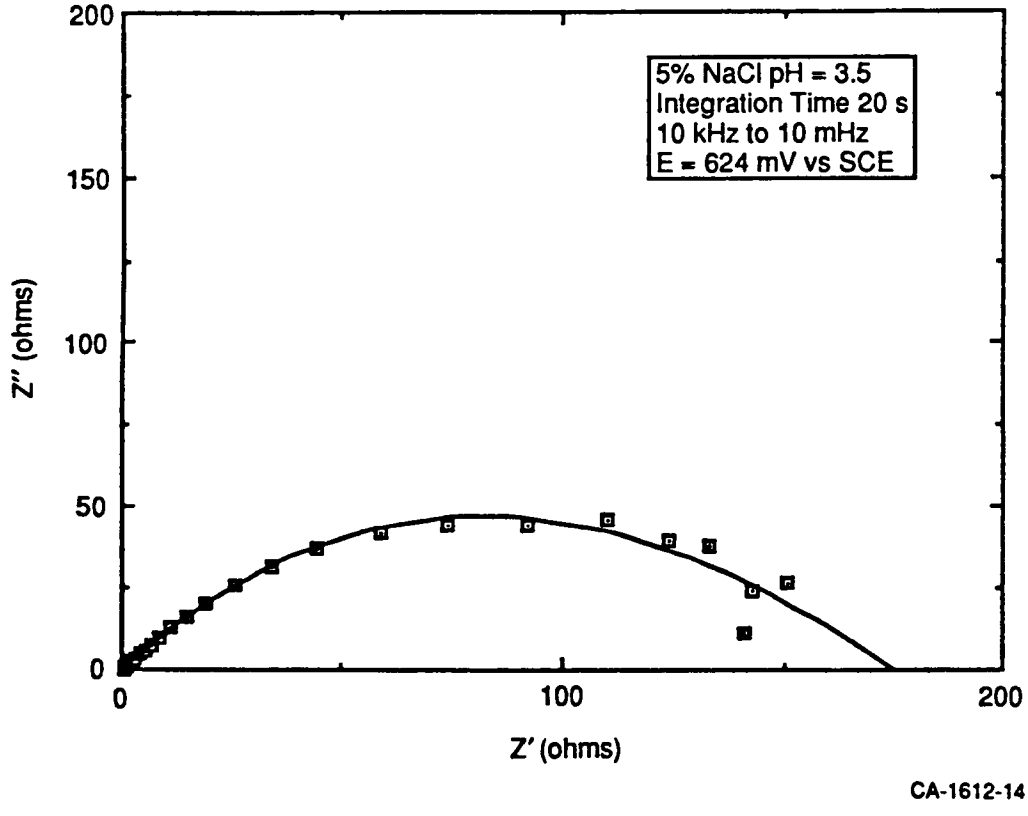

Figure 17. AC impedance plot for the uncoated bar.

Figure 18 shows the impedance plot of a silicon-coated bar prepared at 500°C. The AC response forms a semicircle, and the polarization resistance was approximately 280 Ω. This coating was more compact, and fewer pinholes spots of corrosion products were observed. Those pinholes that were observed, however, were located at the cut ends of the rebar. The cut end makes up an characteristically large area of the rebar in these small research samples. Thus, the cut ends of the rebar were masked off in later experiments to prevent these higher levels of grain boundaries and impurities than are typically observed in the bulk surface from interfering with AC measurements.

Figure 19 shows the AC response of a rebar sample coated with a mixture of silicon and titanium. The coating shows a marked improvement in corrosion resistance, as illustrated by the increase in the polarization resistance, although the ends were sealed with epoxy resin to prevent interference from the unrepresentative end sections. The coating also did not show any areas where corrosion had occurred through pinholes or areas of high porosity.

The polarization resistance data was used to estimate corrosion rates using known Tafel coefficients. Table 4 shows the R_p and corrosion rate data for three rebar samples. Clearly, both silicon and silicon-titanium coatings lower the corrosion rate substantially. The silicon-titanium coating lowers the corrosion rate to approximately 1/15 of the uncoated bar.

Table 4. Rate of rebar corrosion in 5% NaCl at pH 3.5.

Sample	Rp Ωcm^{-2}	Corrosion Rate (mils per year)
Uncoated	540	73
Coated Si/500°C	840	47
Coated Si/Ti Doped	2850	4.6

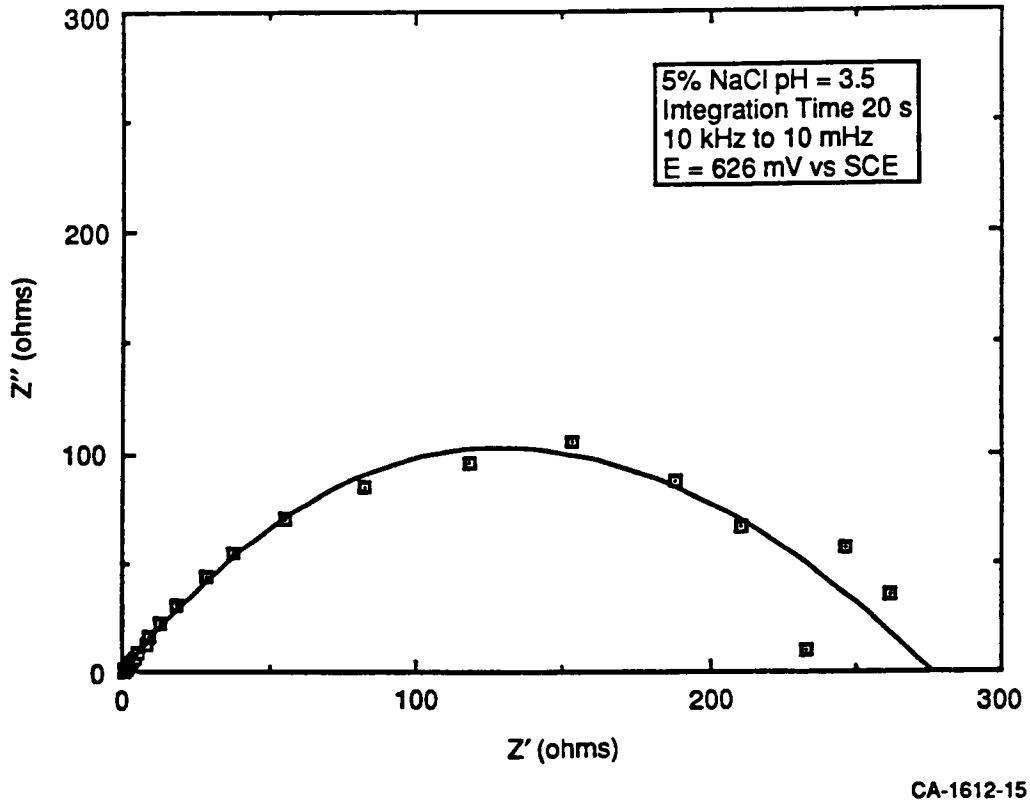

Figure 18. AC impedance plot for a silicon-coated sampled prepared at 500°C.

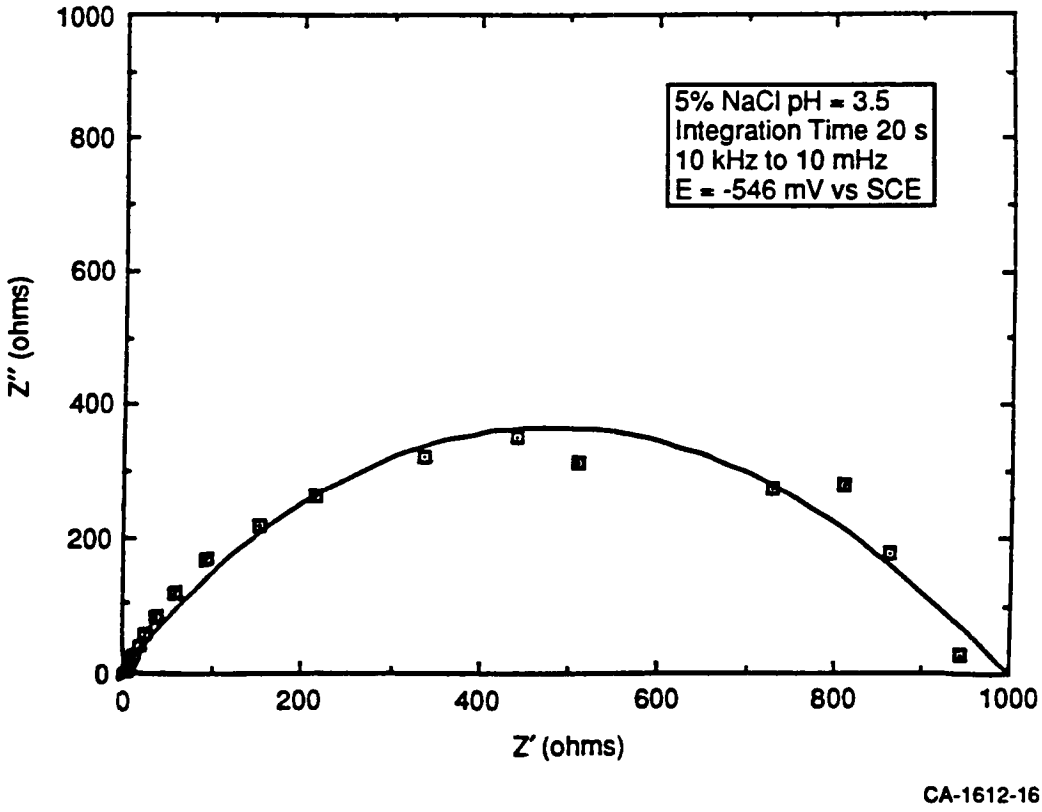

Figure 19. AC impedance plot for a silicon-titanium-coated rebar sample.

3

DISCUSSION

As the HCl enters the bed, it reacts with the Si and Ti particles to produce Si-Cl, SiCl-H, or Ti-Cl species. Equilibrium between the solid-particle phase and the surrounding gas phase is approached closely in the bed. As the Fe is placed in contact with the bed, a very large gradient in the thermodynamic activities of Si and/or Ti between the gas phase and the Fe surface is established. Thus, Si and/or Ti is transferred from the particle bed to the substrate surface. Silicon diffuses into the Fe interstices, forming a solid solution, corresponding to α-Fe in the phase diagram (Figure 20) Ti however, diffuses less readily and remaining near the surface. This increase in Si/Ti concentration at the surface competes with a corresponding diffusion of Fe from the bulk to the coating.

For silicon coatings, observed first the formation of α-Fe at temperatures below 500°C, followed by the formation of Fe_3Si after 5 minutes at 500°C and that of FeSi and even Si at higher temperatures or longer times. Cabrera et al. [5] obtained similar results when using SiH_4 for coating. Using thermogravimetry, they also observed a rapid linear Si uptake, followed by saturation and diffusion-limited uptake.

As the Si concentration increases, the first iron silicide precipitates. Because of the relative stability of Fe_3Si (-25 kJ mol), we expected this phase to rapidly cover the Fe surface and indeed that was the case. According to Murarka (12), the silicides with higher Si content have a more negative heat of formation (Fe_3Si = -7.5; Fe_5Si_3 = -11.7; FeSi = -17.6; $FeSi_2$ = -19.4 kcal/metal atom), indicating a tendency of the silicide to increase its Si content. In the presence of excess iron, the phase closest to iron (in the phase diagram) is typically formed (12).

Therefore, our findings that the silicide coatings grow in a layered mode with progressively richer silicon phases on the outer surface seem to follow the thermochemical scale. Even when such layers are formed, the driving force for Si deposition at the gas silicide interphase is still appreciable, because the Si in the bed pegs the activity of Si to unity. Therefore, silicon deposition proceeds through the FeSi phase, the $FeSi_2$ phase, and all the way to pure Si deposits, as we observed at T > 650°C. The differences in densities and chemical reactivity between the silicide

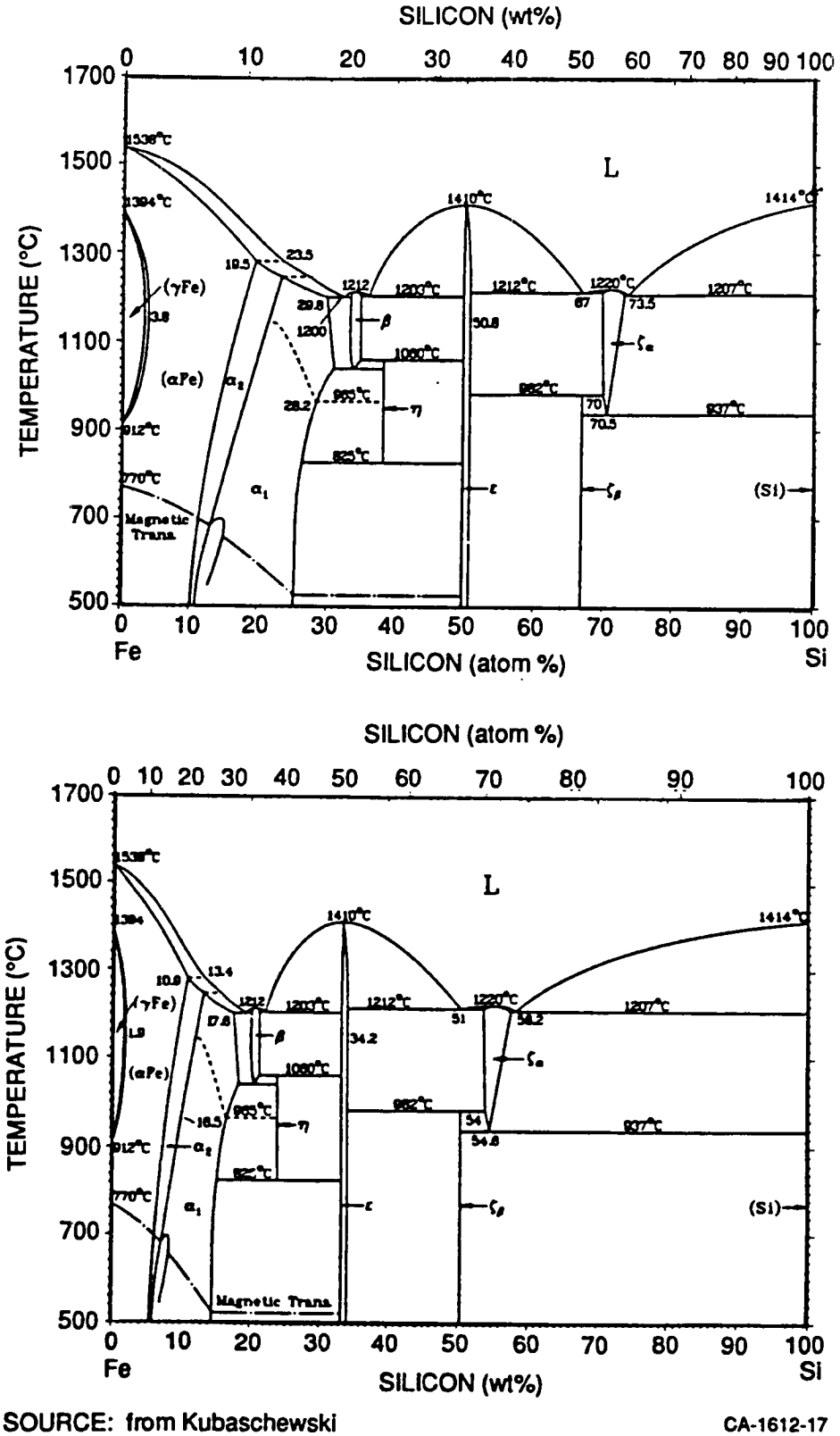

SOURCE: from Kubaschewski

CA-1612-17

Figure 20. Fe-Si binary alloy phase diagrams.

phases seem to be the main reason for the observed morphology. The difference in the interdiffusion rates of Fe and Si in iron silicide might be responsible for pore formation in the diffusion layer. The formation of pores in the outer corrugated silicide layer at high temperatures (>650°C) may be due to the formation of volatile $FeCl_2$ as proposed by Klam et al. (13). We however, deposited at much lower temperatures (600°C versus 750° to 1100°C) than Klam et al., and the vapor pressure of this species is very low at the lower temperatures (Figure 2). More characterization work will be required to establish the mechanism of silicide formation.

The Si-Ti coatings show the best corrosion protection of all the coatings, even for thin layers containing only 2.5% of Si and Ti. From the X-ray diffraction results (no intermetallic phases detected) and the published ternary phase diagrams for the Fe-Si-Ti system (14,15), we concluded that both elements diffuse into the Fe lattice, strengthening it and protecting it from corrosion. With thicker coatings we expect Ti to show a tendency to pile up at the surface, thus conferring good protection from corrosion while keeping the surface flexible enough to survive bending.

The cost of coating steel rebars with a Si-Ti based alloy can be estimated by comparison with that of conventional polymer coatings. In conventional coating, the rebar is sand-blasted, preheated, coated in a fluidized bed, and cooled down. In the new proposed Si-Ti coating, the process will be basically the same with the exception that, the fluidized bed will contain Si-Ti powder mixtures and it will operate at 550°C. The total fixed capital for a plant producing 16 million linear ft/yr of polymer-coated, 0.5-in-diameter rebars is about 1.1 million dollars. For a 8 mils polymeric coating, at a cost of $3/lb of polymer powder, the material cost is about $300,000/yr. Other direct costs and operating costs bring the annual operating cost to about 1.7 million dollars, and the cost of coating with polymers to about $0.10/ft. of rebar. By comparison, the low cost of Si ($0.5/lb) and Ti ($3.5/lb) and the need to use less than 0.1 mil thick coatings, results in a comparatively negligible materials cost. The estimated approximate cost for a Si-Ti based coating will be $0.08 ft of rebar if our assumptions are correct.

4

Conclusions and Recommendations

It can be concluded that

(a) Si or Si-Ti diffusion layer can be formed on steel rebars by chemical vapor deposition in fluidized bed reactors to produce a corrosion resistant bar.

(b) The corrosion rate of steel rebars in aqueous acidic environments can be reduced by half using Si based coatings, and to one tenth using Si-Ti-based coatings obtained at 550°C

(c) Thick silicide coatings obtained above 650°C are multilayered and the top layers often spall and debond.

(d) Thin Si-based coatings and Si-Ti coatings are very adherent, compact, and practically scratch proof, and can be bent without cracking or delaminating.

This technique can be engineered directly into the currently available polymeric coating lines by substituting the polymer-FBR by the CVD-FBR. Preliminary cost estimates for a plant producing 16 million linear feet per year, indicate that the cost of coating with a Si-Ti coating would be less than the cost of currently used polymeric coatings.

We therefore recommend pursuing this approach vigorously because it can provide a very protective coating at a low cost.

5

References

1. Transportation Research Record 1041, Transportation Research Board, National Research Council, Washington, DC, 1985.

2. M. G. Fontana and N. D. Greene, *Corrosion Engineering*, McGraw-Hill, New York, 1978.

3. G. Wahl and B. Furst, *Metals Handbook*, T. Lyman (Ed.), ASM, Metals Park, Ohio, 1961.

4. D. R. Holmes and A. Rahmel (Eds.), *Materials and Coatings of Resistant High Temperature Corrosion*, Applied Science Publishers Ltd., London (1978), pp. 333-352.

5. A. Cabrera et al., J. Mater. Res. 6 (1991); U.S. Patents 4,714,632 and 4,822,642, and references therein.

6. A. Cabrera et al., U.S. Patent 4,822,642, April 18, 1989, and references therein.

7. Angel Sanjurjo et al., Surf. Coatings Technol. 39/40 (1989) 691.

8. A. Cabrera and J. K. Kirner, Surf. Coatings Technol. 39/40 (1989) 43.

9. A. Sanjurjo et al., Surf. Coatings Technol. 49 (1991) 103-110.

10. G. H. Wagner, U.S. Patent 2,499,099, 28 Feb. 1950.

11. J. L. Falconer and J. A. Schwarz, Catal. Rev. Sci. Eng. 25(2) 193, 141-227.

12. V. Murarka, *Silicides for VLSI Applications*, Academic Press, London (1983), p. 82.

13. C. Klam et al., J. Mater. Sci. 26 (1991) 4945.

14. R. Vogel and W. Schluter, "The Iron Corner of the Iron-Silicon-Titanium System," Arch. Eisenhüttenwes. 12 (1938) 207.

15. G. G. Bentle and W. P. Fishel, Trans. Am. Inst. Min. Metall. Eng., 206 (1956) 1345.

SHRP-IDEA Advisory Committee

Chairman
Mark Yancey
Texas State Department of Highways and Public Transportation

Raymond Decker
University Science Partners, Inc.

Barry J. Dempsey
University of Illinois

Serge Gratch
GMI Engineering and Management Institute

A.M. Shirole
New York State Department of Transportation

Earl C. Shirley
CALTRANS

Richard N. Wright
National Institute of Standards and Technology

Liaisons

William G. Agnew
General Motors Research (retired)

Tom Christison
Alberta Research Council

Lawrence L. Smith
Florida Department of Transportation

Edwin W. Hauser
Arizona State University

Thomas J. Pasko, Jr.
Federal Highway Administration

Robert Spicher
Transporation Research Board